PLOS ONE

RESEARCH ARTICLE

# A novel truncating variant of GLI2 associated with Culler-Jones syndrome impairs Hedgehog signalling

**Fabiola Valenza[1☯], Davide Cittaro[2☯], Elia Stupka[2,3], Donatella Biancolini[2], Maria Grazia Patricelli[4], Dario Bonanomi[1], Dejan Lazarević[2]***

**1** Molecular Neurobiology Laboratory, Division of Neuroscience, IRCSS San Raffaele Scientific Institute, Milan, Italy, **2** Centre for Translational Genomics and Bioinformatics, IRCSS San Raffaele Scientific Institute, Milan, Italy, **3** Dana-Farber Cancer Institute, Harvard Medical School, Boston, MA, United States of America, **4** Molecular Biology and Citogenetics, IRCSS San Raffaele Scientific Institute, Milan, Italy

☯ These authors contributed equally to this work.
* lazarevic.dejan@hsr.it



OPEN ACCESS

**Citation:** Valenza F, Cittaro D, Stupka E, Biancolini D, Patricelli MG, Bonanomi D, et al. (2019) A novel truncating variant of GLI2 associated with Culler-Jones syndrome impairs Hedgehog signalling. PLoS ONE 14(1): e0210097. https://doi.org/10.1371/journal.pone.0210097

**Editor:** Jingwu Xie, Indiana University School of Medicine, UNITED STATES

**Received:** July 12, 2018

**Accepted:** December 16, 2018

**Published:** January 10, 2019



**Data Availability Statement:** All relevant data are within the paper and its Supporting Information files. Raw sequencing data and individual genotypes ar not available due to restrictions in the patient informed consent. All relevant data for the article is available upon request to Dott. Giorgio Presepio (giorgio.presepio@grupposandonato.it), DPO due to lack of informed consent by patients and restrictions imposed by the Comitato Etico Ethics Committee (http://comitatoetico.hsr.it/Contatti/index.html).

## Abstract

### Background

GLI2 encodes for a transcription factor that controls the expression of several genes in the Hedgehog pathway. Mutations in GLI2 have been described as causative of a spectrum of clinical phenotypes, notably holoprosencephaly, hypopituitarism and postaxial polydactyl.

### Methods

In order to identify causative genetic variant, we performed exome sequencing of a trio from an Italian family with multiple affected individuals presenting clinical phenotypes in the Culler-Jones syndrome spectrum. We performed a series of cell-based assays to test the functional properties of mutant GLI2.

### Results

Here we report a novel deletion c.3493delC (p.P1167LfsX52) in the C-terminal activation domain of GLI2. Functional assays confirmed the pathogenicity of the identified variant and revealed a dominant-negative effect of mutant GLI2 on Hedgehog signalling.

### Conclusions

Our results highlight the variable clinical manifestation of GLI2 mutations and emphasize the value of functional characterisation of novel gene variants to assist genetic counselling and diagnosis.

## Introduction

The Hedgehog (Hh) family of secreted morphogens control cell proliferation, differentiation and patterning during embryo development [1]. In humans, gene mutations in molecular

**Funding:** This work was supported by theEuropean Research Council under the European Union's Seventh Framework Programme (FP7/2007-2013)/ ERC-StG 335590 NEVAI (https://cordis.europa.eu/project/rcn/192565_en.html); Career Development Award of the Giovanni Armenise-Harvard Foundation (http://www.armeniseharvard.org/portfolio-articoli/dario-bonanomi/) and 5x1000 from Italian Ministry of Health (http://www.salute.gov.it/portale/temi/p2_6.jsp?lingua=italiano&id=4227&area=Ricerca%20sanitaria&menu=vuoto). The funders had no role in study design, data collection and analysis, decision to publish, or preparation of the manuscript.

**Competing interests:** The authors have declared that no competing interests exist.

components of the Hh pathway are associated with a number of congenital malformations or syndromes, characterized by abnormal development of brain structures, limbs and midline face, such as Holoprosencephaly (HPE), Greig cephalopolysyndactyly syndrome, Pallister-Hall Syndrome, Culler-Jones syndrome, and non-syndromic polydactylies [2]. Besides its key roles in embryogenesis, Hh signaling remains active in some adult tissues, contributing to organ homeostasis and regeneration [3], whereas aberrant activation of the pathway occurs in several human cancers, including basal cell carcinoma and medulloblastoma [4].

All three vertebrate Hh ligands, Sonic hedgehog (*SHH*), Indian hedgehog and Desert hedgehog activate the same signal transduction pathway but operate in different tissues and organs. In the embryo, a concentration gradient of SHH, the most potent and best studied member of the family, specifies the identity of ventral neuron types along the entire rostral-caudal length of the central nervous system. SHH functions in the limb bud to define number, position and character of the digits [5], and contributes to the development of the pituitary gland [6], cerebellum [7,8], midbrain [9], eye [10] and face [11].

The effects of "canonical" Hh pathway are mediated by the GLI family of transcription factors (GLI1, GLI2 and GLI3), which control the expression of a number of target genes [12]. The three GLI proteins share a conserved C2H2-type zinc finger DNA-binding domain [13]. In addition, GLI2 and GLI3 possess an N-terminal repressor domain and a C-terminal activator domain, whereas GLI1 functions solely as an activator [14–16]. In the absence of Hh ligand, the membrane receptor Patched1 (PTCH1) inhibits the seven-transmembrane protein Smoothened (SMO) by preventing its access to the primary cilium. In this "off" state, GLI2 and GLI3 are retained in the cytoplasm by SUFU, a main negative regulator of the pathway, and undergo partial proteolytic processing that removes the C-terminal activation domain generating transcriptional repressor forms GLI3R and, to a lesser extent, GLI2R. Upon SHH binding, PTCH1 inhibition of SMO is relieved. As a result, GLI2 and GLI3 are converted into transcriptional activators (GLIA) that translocate into the nucleus to drive expression of target genes, including *GLI1* and *PTCH1*. Generally, GLI2A is the predominant activator of the pathway whereas GLI3R is the major transcriptional repressor, and their relative levels shape the SHH response [17–19].

*GLI2* is a large and highly polymorphic gene, with a number of rare/family-specific heterozygous missense, non-sense, and frameshift mutations detected in individuals presenting with a spectrum of clinical phenotypes that include HPE, craniofacial abnormalities, polydactyly, panhypopituitarism, secondary hypogonadism or isolated growth hormone deficiency [20–24]. The broad and variable range of clinical manifestations may have its origin in the bifunctional transcriptional activity of GLI2 and the complex regulatory feedbacks operating in the Hh signaling pathway, and points to possible modifying effects of additional genetic and environmental factors. Because it may be challenging to interpret the significance and impact of *GLI2* mutations, gene variants need to be functionally characterized to assess their pathogenicity and support genotype-phenotype correlation.

Here, we identify and functionally validate a novel truncating variant in the activation domain of GLI2 linked to a Culler-Jones syndrome phenotype characterized by hypopituitarism, polydactyly and facial dysmorphism in an Italian family.

## Material and methods

### DNA extraction and sequencing

Genomic DNA (gDNA) was extracted from 800 μl of peripheral blood using the automated extractor Maxwell 16 Research System (Promega, Madison, WI, USA); the concentration and high quality of gDNA (A260/280 1.8 to 2.0) was determined using a Nanodrop

Spectrophotometer 1000 (Thermo Fisher Scientific, Wilmington, DE, USA). Library preparation was performed using Illumina Nextera Expanded Rapid Capture Enrichment Exome. Exome sequencing was carried out on Illumina HiSeq 2500 platform (Illumina, Inc. San Diego, CA, USA) using SBS chemistry. Libraries were sequenced in paired end mode, 101 nucleotides long each.

This study was approved by the Institutional Ethical Review Committee, San Raffaele Hospital, Milan, Italy (prot. RARE-DISEASE) and informed consent was obtained from all participants.

## Data analysis

Reads were aligned to reference genome hg19 using bwa aln (v 0.6.2) [25]. Variant calling was performed using GATK Unified Genotyper (v.2.4.9) [26] after Indel Realignment and VQSR according to GATK best practices [27].

Variant effect prediction was performed using SnpEff v3.6 [28] using GRCh37.34 genome version, subsequently variants were annotated to dbSNP v146 and to dbNSFP v2.4 [29] using same suite.

The following chain of filters was applied to the variant set: GATK VQSLOD $>$ 0, predicted change in coding sequence, segregation according to a dominant model, rarity in the population (COMMON = 0 in dbSNP build 137), predicted to be damaging according to SIFT [30] and Polyphen [31]. Genes were prioritized using the Phenolyzer platform [32].

## Expression plasmids

The Human GLI2 cDNA clone was obtained from Addgene (pCS2-hGli2 #17648 [24]) For N-terminal GFP tagging of GLI2, hGLI2 cDNA was inserted at the 3'-end of EGFP in the CMV expression vector pN1-EGFP (Clontech) using standard PCR-cloning. GeneArt Mutagenesis kit (Thermo) was used to introduce the deletion c.3493delC (p.P1167LfsX52) into GFP-tagged wild-type GLI2 expression construct using the following primers:

Forward 5′- CCAGCCAGGTGAAGCCTCCACCTTTCCTCAGGGCAACCTG-3′

Reverse 5′- CAGGTTGCCCTGAGGAAAGGTGGAGGCTTCACCTGGCTGG-3′

## Western blotting

HEK293T cells (AD-293 cell line) were maintained in DMEM supplemented with 10% FBS, 1% L-Glutamine, 1% Penicillin/Streptomycin. Cells transfected with the GFP-tagged constructs or pN1-EGFP control for 36 hrs using Lipofectamine 2000 (Thermo) were lysed on a nutator for 30 min at 4˚C in lysis buffer (NaCl 150 mM, EDTA 2 mM, Tris-HCl pH7.5 50 mM, Triton 1%) supplemented with protease and phosphatase inhibitor cocktails. After clarification by centrifugation at 13,000 g for 10 min at 4˚C, 20 μg of total protein lysate were analyzed by SDS-PAGE followed by immunoblot with rabbit anti-GFP antibody (1:1000; Thermo) and rabbit anti-GAPDH (1:5000; Cell Signaling). Detection was performed by standard chemiluminescence with ECL Plus Western Blotting Substrate (Pierce/Thermo).

## Immunofluorence assays

NIH-3T3 mouse fibroblasts were seeded on glass coverslips in DMEM supplemented with 10% FBS, 1% L-Glutamine, 1% Penicillin/Streptomycin for 24 hrs, prior to treatment with 16 nM SHH (Recombinant mouse SHH C25II N-Terminus, R&D Systems) in DMEM containing 0.5% FBS for 5 hrs. Cells were fixed for 20 min at RT with 4% PFA diluted in PBS and

containing 4% sucrose, washed in PBS, stained with DAPI for 5 min and imaged with a 63x objective on a Leica TCS SP8 confocal microscope.

### Quantitative real-time PCR

NIH-3T3 cells were transfected in 12-well plate format with the indicated plasmids using Lipofectamine 2000 [1 μg DNA:1.5 μl Lipofectamine per well]. After 24 hrs, cells were treated with SHH (16 nM) in DMEM containing 0.5% FBS for 40 hrs. 1 μg of total RNA extracted with Trizol (Thermo) was reverse transcribed into cDNA with M-MLV Reverse Transcriptase using random primers, and analyzed by SYBR green-based real-time quantitative PCR (SYBR Select Master Mix, Thermo) with the following primer sets:

*GAPDH (F 5′- AATGTGTCCGTCGTGGATCTGA-3′; R 5′-AGAAGGTGGTGAAGCAGG CATC-3′)*, *GLI1* (F 5′-TTATGGAGCAGCCAGAGAGA-3′; R 5′- ATTAACAAAGAAGCGG GCTC-3′)

*Ptch1* (F 5′- TGACAAAGCCGACTACATGC-3′; R 5′- AGAGCCCATCGAGTACGCT-3′)

### Luciferase assays

NIH-3T3 were transfected in 24-well plate format using Lipofectamine 2000 with GFP-tagged wild-type GLI2, GLI2$^{MUT}$ or GFP control plasmids along with a 8x-GLI-BS-Luc Firefly luciferase reporter construct containing eight repeats of the GLI binding sequence [16] and a plasmid expressing Renilla luciferase under the CMV promoter for normalization (Promega) in a 3:2:1 ratio (GLI2/mock GFP plasmids:8x-GLI-BS-Luc:Renilla Luc) [600 ng total plasmid DNA:1 μl Lipofectamine per well].24 hrs after transfection, cells were treated with SHH (16nM) in DMEM containing 0.5% FBS for 30 hrs and processed with Dual Luciferase Assay Kit (Promega) for measurement of Firefly and Renilla luciferase activities.

The same plasmids mixed at 2:1:1 ratio (GLI2/mock GFP plasmids:8x-GLI-BS-Luc:Renilla Luc) were electroporated "in-ovo" into neural progenitor cells in the neural tube of HH stage 13–14 chick embryos [33] using a square wave electroporator (BTX). After 24 hrs, the electroporated spinal cords were dissociated with trypsin supplemented with DNase (100U, Sigma) and cells were cultured for 1–2 hrs on PDL (100 μg/ml)/laminin (1 μg/ml)-coated 24-well plate in Neurobasal media containing B27 supplement (Gibco/Thermo Scientific), 2mM L-Glutamine (Gibco/Thermo Scientific), 1% Penicillin/Streptomycin (Gibco/Thermo Scientific), 50 μM Glutamic Acid (Sigma-Aldrich) [34]. Cells were then stimulated with SHH at the indicated concentrations for 24 hrs prior to harvesting and processing with Dual Luciferase Assay Kit (Promega).

## Results

### Clinical phenotype of the patients

Proband is a 6 year old female with neonatal panhypopituitarism (HP:0000871), prominent forehead (HP:0011220), thin upper lip vermilion (HP:0000219), downslanted palpebral fissures (HP:0000494), 2–3 finger syndactyly (HP:0001233), low-set ears (HP:0000369), single median maxillary incisor (HP:0006315), long philtrum (HP:0000343), bilateral postaxial hexadactyly (HP:0006136), choanal atresia (HP:0000453) and anterior pituitary agenesis (HP:0010626). Her father was diagnosed with hypopituitarism (HP:0040075) [hypothyroidism (HP:0000821), growth hormone deficiency (GHD) (HP:0000824)], unilateral hexadactyly (HP:0001162), and ectopic pituitary posterior lobe (HP:0011755). After further investigation, hexadactyly (HP:0001162) was described in the paternal grandfather, while GHD (HP:0000824) and hypopituitarism (HP:0040075) were identified in the paternal uncle who did not exhibit hand anomalies (Fig 1A).

The proband was previously tested negative for mutations in candidate disease-linked genes *POUF1*, *PROP1*, *HESX1*, *LHX3* and *GLI3*.

## Exome sequencing identifies GLI2 as candidate disease gene

Exome sequencing was performed on the trio (Fig 1A) at average target coverage of 30x for each sample (S1 Table). After variant calling, 130 rare or novel variants in 125 genes were found segregating according to a dominant model and affecting coding sequences. Once filtered for putative pathogenicity, 40 variants in 40 genes were retained (S2 Table). Candidate genes were prioritized based on their association with the clinical phenotypes of the patients using Phenolyzer software. This analysis unambiguously identified *GLI2* as the top-scoring gene, while other candidates (*WDR34*, *DPAGT1*, *ASXL1*) already known to be associated with query phenotypes were ranked significantly lower (Fig 1B). Both the proband and her father were found to carry a novel heterozygous mutation caused by the deletion c.3493delC in the *GLI2* gene, leading to a frameshift and premature stop of translation at residue 1218 (p.P1167LfsX52).

## The mutation p.P1167LfsX52 converts GLI2 into a dominant-negative transcriptional repressor

The frameshift mutation c.3493delC in *GLI2* truncates the C-terminal portion of the transactivation domain required for transcriptional activity (p.P1167LfsX52, Fig 2A). To determine whether this truncation alters GLI2 function, we generated GFP-tagged constructs of either wild-type GLI2 or the p.P1167LfsX52 mutant (hereafter $GLI2^{MUT}$) and examined their functional properties using cell-based assays. As predicted, $GLI2^{MUT}$ revealed by western blotting in transfected HEK293 cells was smaller than the wild-type protein (~129kDa vs. 167kDa; ~156kDa vs. 194 kDa after GFP fusion) (Fig 2B). However, the subcellular distribution of $GLI2^{MUT}$ expressed in NIH-3T3 mouse fibroblasts, which respond to SHH, was similar to that of wild-type GLI2: both proteins were found in the cytoplasm as well as the nucleus in untreated cells and accumulated within the nucleus following stimulation with SHH (Fig 2C–2F). Nevertheless, despite normal nuclear targeting, $GLI2^{MUT}$ was unable to induce expression of the transcriptional targets of SHH signaling *GLI1* and *Ptch1*, whose mRNA levels were instead substantially higher in SHH-treated cells overexpressing wild-type GLI2 relative to mock-transfected controls (Fig 2G and 2H).

To directly investigate the effects of the p.P1167LfsX52 mutation on GLI2 transcriptional activity, we assessed the ability of $GLI2^{MUT}$ to stimulate a GLI-dependent reporter construct (8xGliBS-Luc) in which a promoter containing tandem GLI responsive elements drives expression of firefly luciferase upon activation of the Hedgehog pathway [16]. In NIH-3T3 cells, overexpression of wild-type GLI2 increased reporter activity in a ligand-independent manner to an extent comparable to control cells treated with SHH. Conversely, the basal levels of reporter activity were significantly lower in cells transfected with $GLI2^{MUT}$ and did not show the expected increase after SHH stimulation (Fig 2I).

A complementary set of experiments was conducted in primary cultures of neural progenitor cells derived from the chick embryo neural tube electroporated with either wild-type or mutant GLI2 together with the 8xGliBS-Luc reporter. Spinal cord progenitors depend on graded SHH signaling to acquire class-specific molecular identities during embryo development [35] and exhibit reliable dose-dependent responsiveness to SHH in culture (Fig 2J, control). Electroporation of wild-type GLI2 led to robust induction of reporter activity independent of SHH stimulation, whereas $GLI2^{MUT}$ caused a considerable reduction in luciferase levels compared to control cells at all ligand concentrations tested, indicating that the mutant protein suppresses transcription mediated by endogenous GLI factors (Fig 2J).

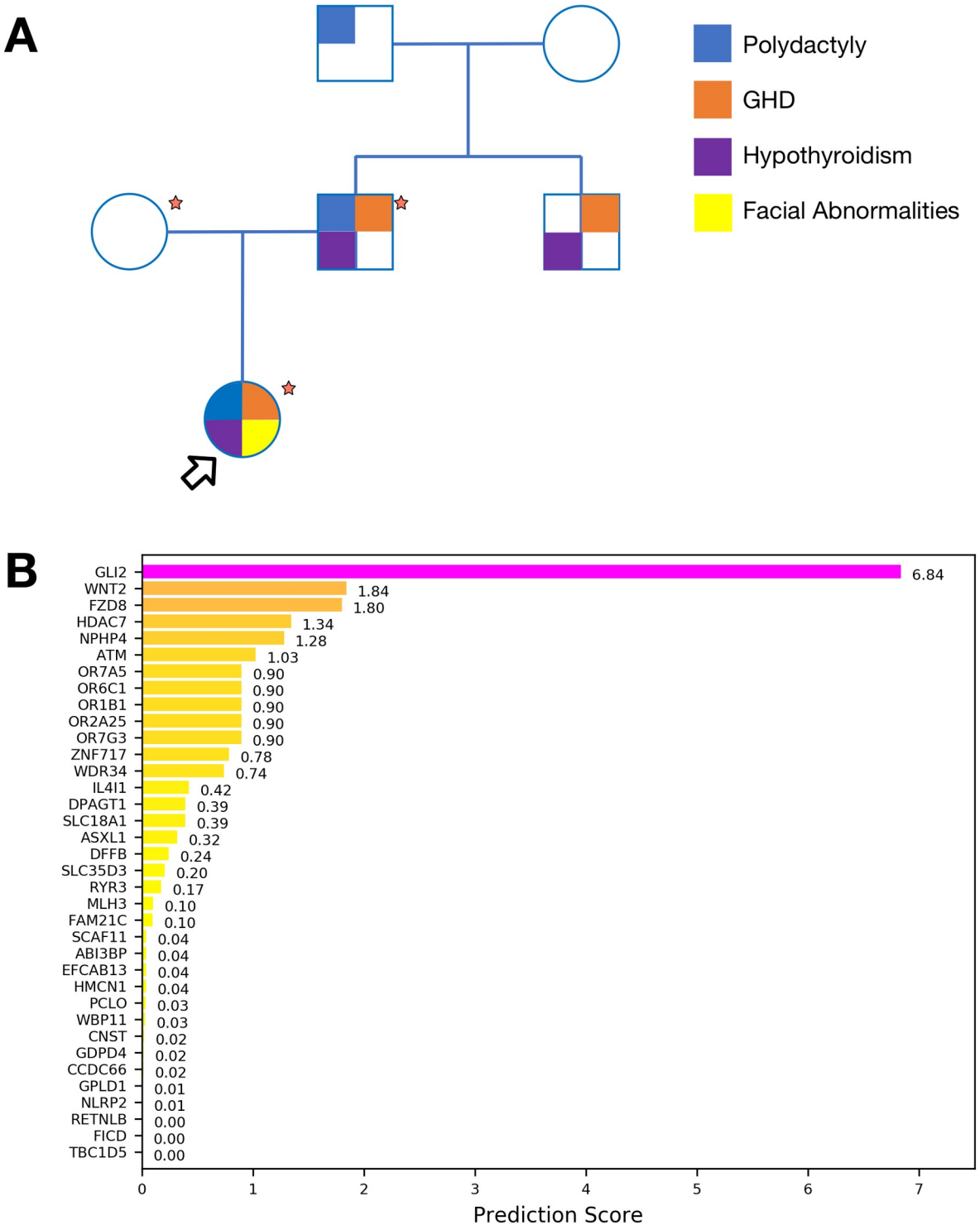


**Fig 1. Exome sequencing identifies *GLI2* as candidate disease gene. (A)** Pedigree of the reported family. Main known phenotypes are mapped to individuals. Samples marked by a red star were available for Exome Sequencing. Proband is indicated with an arrow. **(B)** Bar plot representing prioritization scores obtained with Phenolyzer for genes identified from Exome Sequencing. *GLI2* can be effectively associated with the clinical phenotype.

https://doi.org/10.1371/journal.pone.0210097.g001

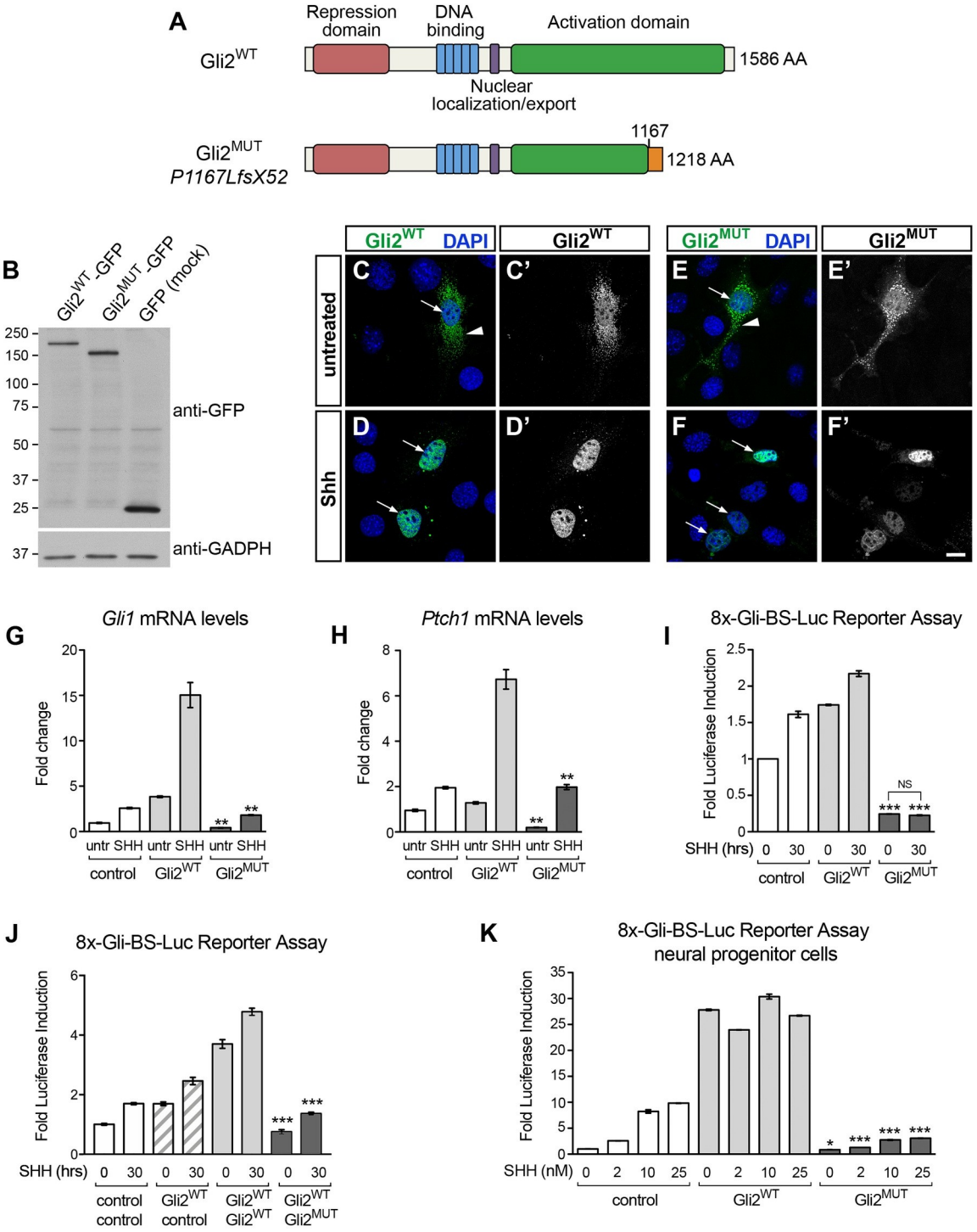


**Fig 2. GLI2 mutant p.P1167LfsX52 lacks transcriptional activity and inhibits Hedgehog-GLI signaling. (A)** Schematic of GLI2 wild-type and p.P1167LfsX52 mutant lacking the C-terminal region of the activation domain. Other functional motifs are intact, including the N-terminal repressor sequence, the zinc finger DNA-binding domain and nuclear localization signal. **(B)** Western blotting of total protein lysates of HEK293 cells transfected with plasmids expressing GFP-tagged wild-type human GLI2 ($GLI2^{WT}$), p.P1167LfsX52 ($GLI2^{MUT}$) or GFP (mock control) revealed with anti-GFP antibody. GADPH is a loading control. **(C-F')** GFP-tagged $GLI2^{WT}$ or $GLI2^{MUT}$ visualized in transfected NIH-3T3 cells before or after stimulation with SHH (16nM) for 5 hrs. The GFP signal extracted from the corresponding merged images is show in C'-F'. Both proteins are found in the cytoplasm (arrowhead) and nucleus (arrow) in untreated cells and become primarily localized to the nucleus after stimulation. Scale bar, 10μm. **(G, H)** Levels of *GLI1* **(G)** and *PTCH1* **(H)** transcripts detected by quantitative-PCR in NIH-3T3 cells expressing GFP-tagged $GLI2^{WT}$, $GLI2^{MUT}$ or GFP control, before and

after treatment with SHH (16nM) for 40 hrs. All conditions are normalized to untreated control cells (mean ± SEM, n = 2). Unpaired *t*-test, (**) $p<0.01$ $GLI2^{MUT}$ vs. $GLI2^{WT}$ either untreated or SHH-treated matching conditions. (**I**) Luciferase-based reporter assay with GLI-responsive construct 8x-Gli-BS-Luc in NIH-3T3 cells transfected with GFP-tagged $GLI2^{WT}$, $GLI2^{MUT}$ or GFP control, before and after treatment with SHH (16nM) for 30 hrs. The expression levels of the reporter gene are measured by luciferase activity. All conditions are normalized to untreated control (mean ± SEM, n = 2). Unpaired *t*-test (***), $p<0.001$ $GLI2^{MUT}$ vs. control either untreated or SHH-treated matching conditions. (NS, non-significant) $p = 0.1264$ $GLI2^{MUT}$ untreated vs. treated. (**J**) Luciferase-based assay with 8x-Gli-BS-Luc reporter in chick spinal cord progenitor cells expressing GFP-tagged $GLI2^{WT}$, $GLI2^{MUT}$ or GFP control, treated with increasing doses of SHH for 24 hrs. All conditions are normalized to untreated control (mean ± SEM, n = 2–4). Unpaired *t*-test, (*) $p = 0.0137$ $GLI2^{MUT}$ vs. control, untreated; (***) $p<0.001$ $GLI2^{MUT}$ vs. control at corresponding SHH concentrations.

https://doi.org/10.1371/journal.pone.0210097.g002

In conclusion, the truncated mutant p.P1167LfsX52 functions as a transcriptional repressor that exerts dominant-negative effects on GLI-dependent gene expression.

## Discussion and conclusions

This study expands the spectrum of *GLI2* mutations reporting a novel heterozygous pathogenic variant (p.P1167LfsX52) that results in autosomal-dominant developmental abnormalities including polydactyly, hypopituitarism, GHD and hypothyroidism.

Functional studies based on cellular assays demonstrated that the frameshift mutation p.P1167LfsX52 truncates the C-terminal transactivation domain of GLI2 generating a transcriptional-repressor form that retains the ability to translocate into the nucleus in response to SHH but exhibits dominant-negative activity. As a result, we observed a significant inhibition of GLI reporter levels in cells expressing GLI2 p.P1167LfsX52, indicating that the activity of wild-type GLI proteins is suppressed by the mutant variant. Dominant-negative activity was reported for other pathogenic variants of *GLI2* with deletions in the activation domain [24]. The inhibitory effect was found to require integrity of the DNA-binding and amino-terminal transcriptional repressor domains [24, 36], which are intact in GLI2 p.P1167LfsX52. To inhibit positive GLI function, C-terminally truncated variants may compete with and displace wild-type GLI2 from target sites and/or form inactive complexes with the activating forms.

While *GLI2* mutations were originally identified in patients with HPE and midline abnormalities, [23, 24], more recently it became clear that *GLI2* variants are often associated with polydactyly, pituitary deficiency and subtle midfacial facial phenotypes rather than patent HPE [20, 21, 37, 38]. The fact that frank HPE is rare in patients with *GLI2* mutations, in contrast to those with *SHH* variants, has suggested that other GLI proteins (GLI1, GLI3) might function redundantly to compensate in part for GLI2 deficiency, in line with studies in compound mutant mice [16, 39, 40]. Likewise, *GLI2*-null mice display normal limb patterning unless *GLI1* is also ablated, and *GLI2/GLI3* double heterozygous mice have a more severe polydactyly than *GLI3* mutants [40]. Interestingly, polydactyly is generally present in patients with more severe *GLI2* variants, including those that disrupt the zinc-finger and transactivation domains [39]. Specifically, individuals with mutations predicted to result in protein truncation are significantly more likely to present both polydactyly and pituitary insufficiency compared to those with non-truncating variants [20].There is striking variability in the phenotypic outcomes of GLI2 mutations even within the same family tree [21–24, 37], ranging from unaffected carriers to patients with craniofacial abnormalities, pituitary phenotypes and polydactyly, either isolated or in combination. In the pedigree examined in this study, hormone deficiencies, but not hand and facial anomalies, were present in all individuals carrying mutant *GLI2*, in support of the recommendation to consider this gene as a primary candidate to screen after endocrinology testing has revealed pituitary insufficiency even in the absence of polydactyly [41]. Incomplete penetrance and variable phenotypes, as also reported in patients with autosomal dominant mutations in other loci linked to HPE or pituitary deficiencies (e.g.,

*SHH*, *SIX3*, *OTX2*, *HESX1*), suggest the contribution of additional genetic variants, epigenetic changes and environmental factors. Despite the pathogenetic role of *GLI2* mutations has already been described, a small number of rare and damaging variants in the same gene can be found in public data from non-dysmorphic individuals such as the Exome Aggregation Consortium [42] or Exome Variant Server [43]. Therefore, systematic functional validation of putative pathogenic variants would be valuable for genetic counseling and patient screening.

## Supporting information

**S1 Table. Exome sequencing statistics.** Main sequencing statistics for each sample. All samples were sequenced at 30x coverage minimum.
(DOCX)

**S2 Table. Selected variants after filtering.** Genomic positions and annotation of variants selected for disease gene prioritization. Only rare, putative damaging variants segregating in the pedigree were selected. Annotation was performed on GRCh37.34 genome version.
(DOCX)

## Acknowledgments

This work was supported by the Career Development Award of the Giovanni Armenise-Harvard Foundation and by the European Research Council under the European Union's Seventh Framework Programme (FP7/2007-2013)/ERC-StG 335590 NEVAI to D. Bonanomi; It was supported by Italian Ministry of Health (5 per mille).

## Author Contributions

**Conceptualization:** Davide Cittaro, Elia Stupka, Maria Grazia Patricelli, Dario Bonanomi, Dejan Lazarević.

**Formal analysis:** Fabiola Valenza, Davide Cittaro, Donatella Biancolini.

**Funding acquisition:** Elia Stupka.

**Investigation:** Fabiola Valenza, Davide Cittaro, Maria Grazia Patricelli, Dario Bonanomi, Dejan Lazarević.

**Project administration:** Dejan Lazarević.

**Resources:** Donatella Biancolini.

**Supervision:** Dario Bonanomi, Dejan Lazarević.

**Writing – original draft:** Fabiola Valenza, Davide Cittaro, Dario Bonanomi, Dejan Lazarević.

**Writing – review & editing:** Fabiola Valenza, Davide Cittaro, Maria Grazia Patricelli, Dario Bonanomi, Dejan Lazarević.

## References

1. Ingham P. W., Nakano Y., & Seger C. (2011). Mechanisms and functions of Hedgehog signalling across the metazoa. Nat Rev Genet, 12(6), 393–406. https://doi.org/10.1038/nrg2984 PMID: 21502959
2. Bale A. E. (2002). Hedgehog signaling and human disease. Annu Rev Genomics Hum Genet, 3, 47–65. https://doi.org/10.1146/annurev.genom.3.022502.103031 PMID: 12142354
3. Petrova R., & Joyner A. L. (2014). Roles for Hedgehog signaling in adult organ homeostasis and repair. Development, 141(18), 3445–3457. https://doi.org/10.1242/dev.083691 PMID: 25183867

4. di Magliano M. P., & Hebrok M. (2003). Hedgehog signalling in cancer formation and maintenance. Nat Rev Cancer, 3(12), 903–911. https://doi.org/10.1038/nrc1229 PMID: 14737121
5. Tickle C. (2006). Developmental cell biology: Making digit patterns in the vertebrate limb. Nat Rev Mol Cell Biol, 7(1), 45–53. https://doi.org/10.1038/nrm1830 PMID: 16493412
6. Treier M., O'Connell S., Gleiberman A., Price J., Szeto D. P., Burgess R., et al. (2001). Hedgehog signaling is required for pituitary gland development. Development, 128(3), 377–386. PMID: 11152636
7. Dahmane N., & Ruiz-i-Altaba A. (1999). Sonic hedgehog regulates the growth and patterning of the cerebellum. Development, 126(14), 3089–3100. PMID: 10375501
8. Wechsler-Reya R. J., & Scott M. P. (1999). Control of neuronal precursor proliferation in the cerebellum by Sonic Hedgehog. Neuron, 22(1), 103–114. PMID: 10027293
9. Agarwala S., Sanders T. A., & Ragsdale C. W. (2001). Sonic hedgehog control of size and shape in midbrain pattern formation. Science, 291(5511), 2147–2150. https://doi.org/10.1126/science.1058624 PMID: 11251119
10. Heavner W., & Pevny L. (2012). Eye development and retinogenesis. Cold Spring Harb Perspect Biol, 4(12), pii: a008391. https://doi.org/10.1101/cshperspect.a008391 PMID: 23071378
11. Xavier G. M., Seppala M., Barrell W., Birjandi A. A., Geoghegan F., & Cobourne M. T. (2016). Hedgehog receptor function during craniofacial development. Dev Biol, 415(2), 198–215. https://doi.org/10.1016/j.ydbio.2016.02.009 PMID: 26875496
12. Riobo N. A., & Manning D. R. (2007). Pathways of signal transduction employed by vertebrate Hedgehogs. Biochem J, 403(3), 369–379. https://doi.org/10.1042/BJ20061723 PMID: 17419683
13. Kinzler K. W., Ruppert J. M., Bigner S. H., & Vogelstein B. (1988). The GLI gene is a member of the Kruppel family of zinc finger proteins. Nature, 332(6162), 371–374. https://doi.org/10.1038/332371a0 PMID: 2832761
14. Dai P., Akimaru H., Tanaka Y., Maekawa T., Nakafuku M., & Ishii S. (1999). Sonic Hedgehog-induced activation of the Gli1 promoter is mediated by GLI3. J Biol Chem, 274(12), 8143–8152. PMID: 10075717
15. Ruiz-i-Altaba A. (1999). Gli proteins encode context-dependent positive and negative functions: implications for development and disease. Development, 126(14):3205–3216 PMID: 10375510
16. Sasaki H., Nishizaki Y., Hui C., Nakafuku M., & Kondoh H. (1999). Regulation of Gli2 and Gli3 activities by an amino-terminal repression domain: implication of Gli2 and Gli3 as primary mediators of Shh signaling. Development, 126(17), 3915–3924. PMID: 10433919
17. Briscoe J., & Thérond P. P. (2013). The mechanisms of Hedgehog signalling and its roles in development and disease. Nat Revi Mol Cell Biol, 14(7), 416–429.
18. Eggenschwiler J. T., & Anderson K. V. (2007). Cilia and developmental signaling. Annu Rev Cell Dev Biol, 23(1), 345–373.
19. Hui C.-C., & Angers S. (2011). Gli proteins in development and disease. Annu Rev Cell Dev Biol, 27, 513–537. https://doi.org/10.1146/annurev-cellbio-092910-154048 PMID: 21801010
20. Bear K. A., Solomon B. D., Antonini S., Arnhold I. J. P., França M. M., Gerkes E. H., et al. (2014). Pathogenic mutations in GLI2 cause a specific phenotype that is distinct from holoprosencephaly. J Med Genet, 51(6), 413–418. https://doi.org/10.1136/jmedgenet-2013-102249 PMID: 24744436
21. França M. M., Jorge A. A. L., Carvalho L. R. S., Costalonga E. F., Vasques G. A., Leite C. C., et al. (2010). Novel heterozygous nonsense GLI2 mutations in patients with hypopituitarism and ectopic posterior pituitary lobe without holoprosencephaly. J Clin Endocrinol Metab, 95(11), E384–91. https://doi.org/10.1210/jc.2010-1050 PMID: 20685856
22. Paulo S. S., Fernandes-Rosa F. L., Turatti W., Coeli-Lacchini F. B., Martinelli C. E., Nakiri G. S., et al. (2015). Sonic Hedgehog mutations are not a common cause of congenital hypopituitarism in the absence of complex midline cerebral defects. Clin Endocrinol (Oxf), 82(4), 562–569.
23. Roessler E., Du Y.-Z., Mullor J. L., Casas E., Allen W. P., Gillessen-Kaesbach G., et al. (2003). Loss-of-function mutations in the human GLI2 gene are associated with pituitary anomalies and holoprosencephaly-like features. Proc Natl AcadSci U.S.A., 100(23), 13424–13429.
24. Roessler E., Ermilov A. N., Grange D. K., Wang A., Grachtchouk M., Dlugosz A. A., et al. (2005). A previously unidentified amino-terminal domain regulates transcriptional activity of wild-type and disease-associated human GLI2. Hum Mol Genet, 14(15), 2181–2188. https://doi.org/10.1093/hmg/ddi222 PMID: 15994174
25. Li H., & Durbin R. (2010). Fast and accurate long-read alignment with Burrows-Wheeler transform, Bioinformatics, 26(5), 589–595. https://doi.org/10.1093/bioinformatics/btp698 PMID: 20080505

26. Mckenna A., Hanna M., Banks E., Sivachenko A., Cibulskis K., Kernytsky A., et al. (2010). The Genome Analysis Toolkit: a MapReduce framework for analyzing next-generation DNA sequencing data. Genome Res, 20(9), 1297–1303. https://doi.org/10.1101/gr.107524.110 PMID: 20644199

27. DePristo M. A., Banks E., Poplin R., Garimella K. V., Maguire J. R., Hartl C., et al. (2011). A framework for variation discovery and genotyping using next-generation DNA sequencing data. Nat Genet, 43(5), 491–498. https://doi.org/10.1038/ng.806 PMID: 21478889

28. Cingolani P., Platts A., Wang L. L., Coon M., & Nguyen T. (2012). A program for annotating and predicting the effects of single nucleotide polymorphisms, SnpEff: SNPs in the genome of Drosophila melanogaster strain w1118; iso-2; iso-3. Fly, 6(2), 80–92 https://doi.org/10.4161/fly.19695 PMID: 22728672

29. Liu X., Jian X., & Boerwinkle E. (2013). dbNSFP v2.0: A Database of Human Non-synonymous SNVs and Their Functional Predictions and Annotations. Hum Mutat, 34(9), E2393–E2402. https://doi.org/10.1002/humu.22376 PMID: 23843252

30. Kumar P., Henikoff S., & Ng P. C. (2009). Predicting the effects of coding non-synonymous variants on protein function using the SIFT algorithm. Nat Protoc, 4(8), 1073–1081.

31. Adzhubei I. A., Schmidt S., Peshkin L., Ramensky V. E., Gerasimova A., Bork P., et al. (2010). A method and server for predicting damaging missense mutations. Nat Methods, 7(4), 248–249. https://doi.org/10.1038/nmeth0410-248 PMID: 20354512

32. Yang H., Robinson P. N., & Wang K. (2015). Phenolyzer: phenotype-based prioritization of candidate genes for human diseases. Nat Methods, 12(9), 841–843. https://doi.org/10.1038/nmeth.3484 PMID: 26192085

33. Hamburger V., & Hamilton H. L. (1992). A series of normal stages in the development of the chick embryo. 1951. Dev Dyn, 195(4), 231–272 https://doi.org/10.1002/aja.1001950404 PMID: 1304821

34. Bonanomi D., Chivatakarn O., Bai G., Abdesselem H., Lettieri K., Marquardt T., et al. (2012). Ret is a multifunctional coreceptor that integrates diffusible- and contact-axon guidance signals. Cell, 148(3), 568–582. https://doi.org/10.1016/j.cell.2012.01.024 PMID: 22304922

35. Briscoe J., Pierani A., Jessell T. M., & Ericson J. (2000). A homeodomain protein code specifies progenitor cell identity and neuronal fate in the ventral neural tube. Cell, 101(4), 435–445. PMID: 10830170

36. Flemming G. M. C., Klammt J., Ambler G., Bao Y., Blum W. F., Cowell C., et al. (2013). Functional characterization of a heterozygous GLI2 missense mutation in patients with multiple pituitary hormone deficiency. J Clin Endocrinol Metab, 98(3), E567–75. https://doi.org/10.1210/jc.2012-3224 PMID: 23408573

37. Rahimov F., Ribeiro L. A., de Miranda E., Richieri-Costa A., & Murray J. C. (2006). GLI2 mutations in four Brazilian patients: how wide is the phenotypic spectrum? Am J Med Genet, 140(23), 2571–2576. https://doi.org/10.1002/ajmg.a.31370 PMID: 17096318

38. Kordaß U., Schröder C., Elbracht M., Soellner L., & Eggermann T. (2015). A familial GLI2 deletion (2q14.2) not associated with the holoprosencephaly syndrome phenotype. Am J Med Genet, 167A(5), 1121–1124. https://doi.org/10.1002/ajmg.a.36972 PMID: 25820550

39. Arnhold I. J. P., França M. M., Carvalho L. R., Mendonca B. B., & Jorge A. A. L. (2015). Role of GLI2 in hypopituitarism phenotype. J Mol Endocrinol, 54(3), R141–50. https://doi.org/10.1530/JME-15-0009 PMID: 25878059

40. Park H. L., Bai C., Platt K. A., Matise M. P., Beeghly A., Hui C. C., et al. (2000). Mouse Gli1 mutants are viable but have defects in SHH signaling in combination with a Gli2 mutation. Development, 127(8), 1593–1605. PMID: 10725236

41. Bear K. A., & Solomon B. D. (2015). GLI2 mutations typically result in pituitary anomalies with or without postaxial polydactyly. Am J Med Genet, 167A(10), 2491–2492. https://doi.org/10.1002/ajmg.a.37160 PMID: 25974718

42. Lek M., Karczewski K. J., Minikel E. V., Samocha K. E., Banks E., Fennell T., et al. (2016). Analysis of protein-coding genetic variation in 60,706 humans. Nature, 536(7616), 285–291. https://doi.org/10.1038/nature19057 PMID: 27535533

43. Fu W., O'Connor T. D., Jun G., Kang H. M., Abecasis G., Leal S. M., et al. (2012). Analysis of 6,515 exomes reveals the recent origin of most human protein-coding variants. Nature, 493(7431), 216–220. https://doi.org/10.1038/nature11690 PMID: 23201682